Energy management and stochastic operations planning for electrified container terminals with uncertain energy supply and demand

Stoter, Jasper; Tang, Xinyu; Cvetkovic, Milos; Palensky, Peter; Polinder, Henk; Iris, Çağatay; Schulte, Frederik

DOI
10.1016/j.jclepro.2025.146383

Publication date
2025

Document Version
Final published version

Published in
Journal of Cleaner Production

Journal of Cleaner Production 527 (2025) 146383

Contents lists available at ScienceDirect

Journal of Cleaner Production

journal homepage: www.elsevier.com/locate/jclepro

Energy management and stochastic operations planning for electrified container terminals with uncertain energy supply and demand

Jasper Stoter [a], Xinyu Tang [b,*], Milos Cvetkovic [c], Peter Palensky [c], Henk Polinder [b], Çağatay Iris [d], Frederik Schulte [b]

[a] Emmett Green, Kanaalweg 4, Delft, 2628 EC, The Netherlands
[b] Faculty of Mechanical Engineering, Delft University of Technology, Mekelweg 2, Delft, 2628 CD, The Netherlands
[c] Faculty of Electrical Engineering, Mathematics and Computer Science, Delft University of Technology, Mekelweg 4, Delft, 2628 CD, The Netherlands
[d] School of Management, University of Liverpool, Chatham Building, Chatham Street, Liverpool, L69 7ZH, United Kingdom

ARTICLE INFO

Keywords:
Container terminal
Energy consumption management
Decarbonized ports
Demand response
Stochastic programming

ABSTRACT

Rising energy expenses, the shift towards renewable sources, and grid congestion considerably affect the operations of container terminals. To tackle these challenges, it is necessary to implement energy-aware integrated operational planning which considers related uncertainties. This work proposes a two-stage stochastic mixed integer programming model to optimize container terminal operations planning and demand-responsive energy management. To this end, energy consumption is shifted whenever operationally possible and economically beneficial. We solve the proposed model by developing a dedicated progressive hedging algorithm. Operations considered in this model include vessel scheduling at berths, temperature control of refrigerated containers, and allocation of handling capacity of quay cranes, yard cranes, and automated guided vehicles to serve each vessel. Various scenarios for vessel arrival times and electricity prices are explored representing the uncertainty of energy demand and supply, respectively, based on a case study of the Altenwerder container terminal in Hamburg. Our results suggest potential cost savings of 5.9 per cent on average with a single energy price based on a long-term contract and 13.2 per cent when applying varying real-time electricity prices based on wholesale market rates. These findings underscore the substantial potential of demand response strategies for (electrified) container terminal operations.

1. Introduction

Electricity prices have been volatile in recent years. Between 2019 and 2022, the average electricity price in Europe increased from 38 €/MWh to 235 €/MWh, representing an increase of 518% (ENTSO-E, 2025). This price surge has resulted in higher operational costs for container terminals, particularly those with a high level of electrification, which have been significantly impacted by the rising electricity prices. Challenges related to the transition to renewable energy sources and limited grid capacity in many port regions further aggravate this situation.

Container terminal operators can reduce their energy costs (and ensure energy supply) by implementing a demand response (DR) program. DR program serves as a rationing system to change the power consumption of consumers to better match the demand for power with the supply. Rationing is usually accomplished by price incentives to shift consumption from higher-price periods to lower-price periods. The energy consumption is adjusted through real-time energy prices in DR system, which is more flexible than single energy prices in long-term contracts signed by container terminals to hedge against future price risks and uncertainty. By implementing demand response programs to strategically manage their energy consumption, container terminals can effectively lower energy costs.

The energy demand at a port primarily depends on logistics processes at the port system. Logistics processes within a port are uncertain, leading to complex operations planning with uncertain energy demand. Energy consumption fluctuates significantly throughout the day, depending on the scheduling (Bakar et al., 2021). Terminal operators currently possess limited knowledge about energy consumption patterns. Unlike other industries, container terminals lack continuous and recurring production cycles (Grundmeier et al., 2014). Instead, daily processes in container terminals are highly dynamic depending on

* Corresponding author.
E-mail addresses: jasper.stoter@outlook.com (J. Stoter), X.Tang-3@tudelft.nl (X. Tang), M.Cvetkovic@tudelft.nl (M. Cvetkovic), P.Palensky@tudelft.nl (P. Palensky), H.Polinder@tudelft.nl (H. Polinder), C.Iris@liverpool.ac.uk (Ç. Iris), F.Schulte@tudelft.nl (F. Schulte).

https://doi.org/10.1016/j.jclepro.2025.146383
Received 13 August 2024; Received in revised form 16 July 2025; Accepted 7 August 2025
Available online 24 September 2025

the number of containers and ship arrival patterns (Grundmeier et al., 2014).

Energy management and operations planning considering uncertainty is the research issue that has a great potential for exploration. Several studies concentrate on DR with a single load, while literature focusing on energy-aware integrated planning problems involving multiple energy loads is scarce. Moreover, there is limited work considering the stochastic nature of both energy demand and supply, highlighting the research gap related to energy-aware operational problems with multiple loads considering uncertainty in both supply and demand. To the best of our knowledge, only one work (Iris and Lam, 2021) identified in the literature utilized a stochastic modeling approach that considered multiple scenarios of solar energy production to account for stochastic electricity supply. However, uncertainty in neither port operations nor energy demand has been considered. In our work, we consider uncertain ship arrival time (and resulting uncertainty in energy demand patterns) and uncertain energy prices in particular energy pricing schemes. Moreover, we develop a scenario decomposition algorithm to solve the model efficiently.

This work investigates energy management and energy-aware operations planning in container terminals, in which energy consumption is adjusted by a DR system. The goal of the study is to increase the efficiency of allocating energy resources and arranging operations in container terminals. The main objectives are to minimize schedule and energy-related costs, to demonstrate the impact of stochastic modeling when taking the uncertainty of energy demand and supply and to show the impact of demand response. We optimize the operations planning problem within a container terminal, incorporating the associated energy costs into the objective function. The energy costs of the optimization process include two aspects: the cost of purchasing electricity from the wholesale market and the cost of imbalances resulting from inaccurate consumption predictions. To address the uncertainty of electricity demand and supply, we consider multiple scenarios of ship arrival times and electricity prices. We then conduct computational experiments based on the data from the HHLA Container Terminal Altenwerder (CTA) in Hamburg, Germany. We assess the impact of the uncertainty by comparing the solutions of the stochastic approach to reactive approaches. The impact of DR is presented by comparing the cost savings when applying no energy price, single energy prices and varying prices per hour.

This paper contributes to the field in the following ways:

1. It introduces uncertainty on both energy supply and demand sides when studying operations and energy flows in container terminals. The uncertainty of energy supply and demand is represented by fluctuating energy prices and ship arrival times, respectively.
2. It considers multiple energy loads and integrates planning of Automated Guided Vehicles (AGVs), quay and yard cranes, reefer containers, and ship electricity consumption to derive total energy demand.
3. It introduces a new stochastic programming approach, using scenario decomposition with progressive hedging, and demonstrates it outperforms the reactive approaches through computational experiments based on a terminal in Port of Hamburg, Germany.
4. It quantifies the positive impact of demand response planning in real-time energy pricing schemes through the case study at the terminal in the Port of Hamburg, Germany.

The remainder of this paper is organized as follows. We provide a literature review in Section 2 and define the problem in Section 3. Section 4 establishes the mathematical model for the problem followed by the solution procedure discussed in Section 5. The numerical results and their implications are presented in Section 6. Based on these results, managerial insights are provided in Section 7. Finally, Section 8 summarizes the conclusions and lessons learned from this study.

2. Literature review

Only a small number of studies have dealt with the underexplored area of energy consumption within the container terminals. In a review paper by Iris and Lam (2019b), an overview was provided on operational strategies, technologies, and energy management systems aiming to increase energy efficiency in ports. The authors emphasized the need for future research in operational strategies that incorporated energy-aware planning of operations, particularly in integrated planning problems. Additionally, the importance of an energy management system for balancing energy demand with supply was highlighted. However, this task is challenging due to the fluctuating energy supply from renewable sources, time-variant energy prices, and the difficulty in predicting energy demand resulting from the high operational complexity. Similarly, a review by Bakar et al. (2021) emphasized the growing significance of energy management in future ports. This paper conducted a review of energy-aware planning problems within container terminals. The focus of the review is the on-demand response for integrated planning problems involving multiple energy loads.

Demand response relates to shifting the energy demand to low-demand periods by solving integrated operations planning problems involving multiple energy demand generators. Several studies concentrate on demand response with a single load. In a study by van Duin et al. (2018), the demand response of reefers was considered to lower the peak load. Geerlings et al. (2018) and Kermani et al. (2018) investigated strategies to reduce the peak loads of quay cranes (QCs). These two loads account for the majority of peak demand in container terminals. Another intriguing application of demand response is the use of vehicle-to-grid (V2G) charging for automated guided vehicles (AGVs) within the terminal. Schmidt et al. (2015) explored various business cases for V2G charging with AGVs, and Harnischmacher et al. (2023) further investigated the use of AGVs for frequency containment reserves. Tang et al. (2025) studied smart charging with demand response and energy peak shaving for reefer containers with Internet-of-Things. As the trend towards electrification continues within terminals, ships become a significant electric load through onshore power supply. Yu et al. (2022) performed a multi-objective optimization considering energy-related costs and emissions for berth allocation and quay crane assignment (BACAP) problems. Similarly, He (2016) quantified the impact of energy-aware planning on operational costs by comparing optimization results of an energy-saving strategy (with a constant electricity price) with a time-saving strategy (with no electricity-related cost). Additionally, the effect of energy-aware planning on yard cranes (He et al., 2015a) and automated guided vehicle (He et al., 2015b) scheduling was also investigated. Recent developments in energy system optimization and intelligent energy management, including battery thermal management systems (Oyewola et al., 2024) and real-time grid security (Xiao et al., 2024), underscore the growing importance of integrated control strategies across domains.

Literature specifically focusing on energy-aware integrated planning problems involving multiple energy loads is scarce. Table 1 provides an overview of the most relevant literature, categorized based on the pricing schemes considered for price-based demand response programs. Table 2 presents all the sources of energy demand and supply considered in these studies.

Kanellos (2017, 2019) and other scholars (Kanellos et al., 2019) conducted multiple studies on demand response in container terminals, developing a multi-agent system where different loads communicate with each other. However, these studies do not model detailed operations planning for scheduling activities at the container terminal. Mao et al. (2022) focused on loads within an integrated energy system encompassing electricity, heat, and cooling demands, employing mixed-integer programming optimization. Pu et al. (2020) also addressed an integrated energy system but estimated the total amount of fixed, reducible, and shiftable loads. In the study of Iris and Lam (2021), an integrated

Table 1
Area of focus and pricing scheme of literature closely related to energy-aware integrated planning problems.

Reference	Focus	Uncertainty		Pricing scheme			
		D	S	NP	SP	TOU	RTP
Gennitsaris and Kanellos (2019)	Demand response					√	
Iris and Lam (2021)	Port microgrid		√		√	√	√
Sarantakos et al. (2024)	Energy system	√	√				
Kanellos (2019)	Demand response					√	
Kanellos (2017)	Demand response			√			
Kanellos et al. (2019)	Demand response					√	
Mao et al. (2022)	Integrated energy system				√		√
Pu et al. (2020)	Integrated energy system			√		√	
Xiong et al. (2024)	Port microgrid					√	
Zhao et al. (2024)	Integrated energy system & Demand response	√	√			√	
This paper	Demand response	√	√	√	√		√

Uncertainty: D (Electricity demand), S (Electricity supply).
Pricing scheme: NP (No pricing), SP (Single pricing), TOU (Time-of-use pricing), RTP (Real-time pricing).

Table 2
Energy demand and supply in the literature closely related to energy-aware integrated planning problems.

Reference	Demand							Supply				
	SH	QC	YC	AGV	RE	ESS	Other	EG	WT	PV	ESS	Other
Gennitsaris and Kanellos (2019)	√				√			√	√			
Iris and Lam (2021)	√	√	√		√	√		√		√	√	
Sarantakos et al. (2024)	√	√	√	√	√			√	√	√	√	
Kanellos (2019)	√			√	√			√				
Kanellos (2017)				√	√			√	√			
Kanellos et al. (2019)	√			√	√			√				
Mao et al. (2022)	√				√	√	√	√	√	√	√	√
Pu et al. (2020)						√	√	√				√
Xiong et al. (2024)	√	√	√		√		√	√	√	√	√	√
Zhao et al. (2024)	√	√	√		√		√	√	√			√
This paper	√	√	√	√	√			√				

Demand: SH (Ship), QC (Quay crane), YC (Yard crane), AGV (Automated guided vehicle), RE (Reefer), ESS (Energy storage system).
Supply: EG (Electricity grid), WT (Wind turbine), PV (Photovoltaic panel).

operations planning and energy management problem was solved using stochastic mixed-integer optimization. Our study significantly differs from these studies as we model and obtain detailed demand response through operations planning for AGVs, QCs, YCs, reefer containers and ships with different pricing schemes and uncertainty in both energy demand and supply sides, as presented in Tables 1 and 2.

When proposing energy-aware operations planning, authors often stress the importance of considering the stochastic nature of both energy demand and supply. However, only a very limited number of studies have investigated this topic, with the study of Iris and Lam (2021) as an example. It considered multiple scenarios of solar energy production to account for stochastic electricity supply, without the consideration of uncertainty in the energy demand or port operations. Sarantakos et al. (2024) presented a joint logistics-electric framework for optimal operation and power management of electrified ports, considering multiple uncertainties in the arrival time of vessels, network demand, and renewable power generation. Zhao et al. (2024) constructed a coordinative optimization problem based on the logistics-energy coupling characteristics with the aim of minimizing the port operation cost, the demand response capacity of port flexible loads and the operation constraints of an integrated energy system. Xiong et al. (2024) proposed a joint scheduling method that considers the impact of tidal patterns on the period and intensity of port operations. The method takes advantage of the strong correlations between renewable energy (solar, wind and tidal) and multi-class load to support the port microgrid operator in determining the most cost-effective scheduling of energy supply and flexible loads during port activities. The research gap lies in energy-aware operations (combined with energy management) with multiple loads considering uncertainty in both supply and demand. Our study incorporates uncertain ship arrival times and uncertain energy prices to represent the uncertainty in the energy demand side and supply side, respectively.

3. Problem description

This study aims to assess the potential of demand response by modeling operations planning and energy flows between different components in the container terminal. Different pricing schemes, namely no pricing, single pricing, and real-time pricing, are considered to quantify the impact that demand response has on the operations in the terminal.

To model the problem, we employ a two-stage stochastic programming approach that incorporates uncertainties. Stochastic problems are those optimization problems where some of the parameters of the model are uncertain. Uncertainty can be defined by random variables in the form of probability distributions or densities. A stage of a given planning horizon is a set of consecutive time periods where the realization of one or more stochastic (i.e., uncertain) events take place. At the end of a stage, decisions are taken, considering the specific outcomes of the stochastic events of this and previous stages. In the two-stage stochastic programming, the first stage, known as the "here-and-now" decision, takes place before the values of the uncertain parameters are known. The second stage, the "wait-and-see" decision, is the response to the realization of these uncertain parameters.

Formulation (1) gives the general mathematical formulation of a two-stage stochastic optimization with recourse. In this equation, ξ is the realization of the uncertain parameters. $\mathbb{E}_P$ is the expected value of all realizations of ξ. $f\{\cdot\}$ is the objective function of first stage (F) or second stage (S). $\boldsymbol{A}, \boldsymbol{T}, \boldsymbol{W}$ are the coefficient matrices. $\boldsymbol{b}, \boldsymbol{h}_\xi$ are right-hand-side vectors. $\boldsymbol{x}$ are the first stage decision variables and $\boldsymbol{y}_\xi$ are the second stage decision variables. In linear formulation, $f^F(\boldsymbol{x})$ can be written as $\boldsymbol{c}^\top \boldsymbol{x}$, and $q(\boldsymbol{y}_\xi, \xi)$ can be written as $\sum_\xi p_\xi(\boldsymbol{q}_\xi^\top \boldsymbol{y}_\xi)$ (p_ξ is the probability for each scenario). The linear split-variable formulation of Formulation (1) is shown by Formulation (28).

$$\min_{\boldsymbol{x}} \quad f^F(\boldsymbol{x}) + \mathbb{E}_P[f^S(\boldsymbol{x}, \boldsymbol{y}_\xi, \xi)] \tag{1a}$$

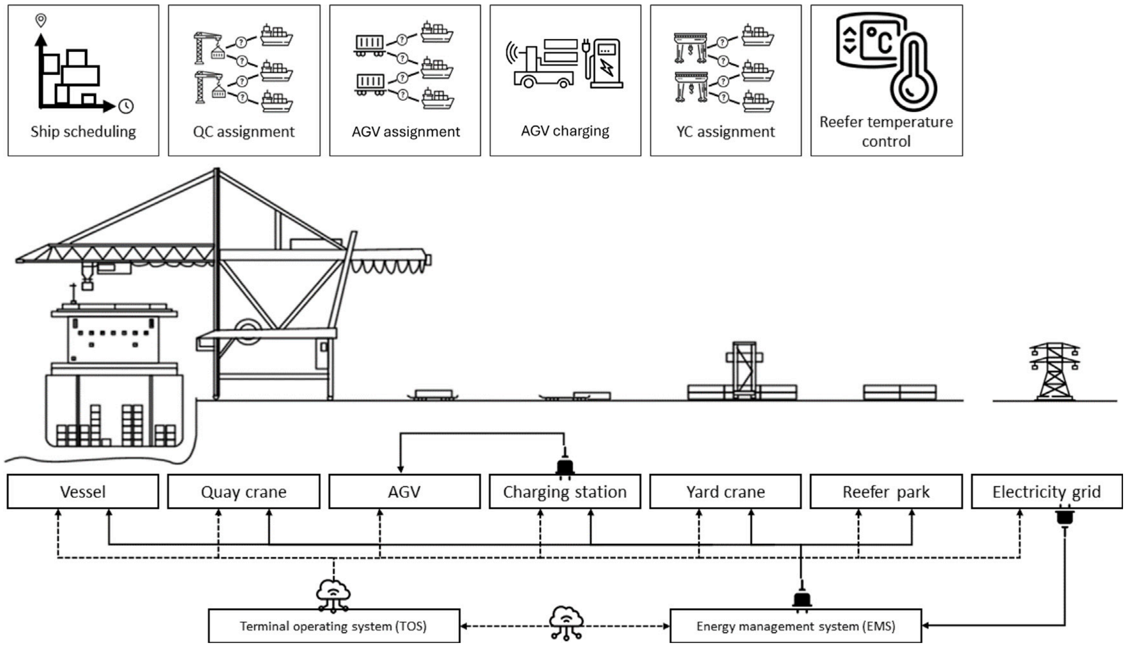

Fig. 1. Overview of operations planning problems, energy flows and information flows in a container terminal.

$$\text{s.t.} \quad \boldsymbol{A}\boldsymbol{x} = \boldsymbol{b}, \tag{1b}$$

$$\text{where} \quad f^S(\boldsymbol{x}, \boldsymbol{y}_\xi, \xi) = \min_{\boldsymbol{y}_\xi} \quad q(\boldsymbol{y}_\xi, \xi), \tag{1c}$$

$$\text{s.t.} \quad \boldsymbol{T}_\xi \boldsymbol{x} + \boldsymbol{W}_\xi \boldsymbol{y}_\xi = \boldsymbol{h}_\xi \tag{1d}$$

In the problem studied, we consider the energy consumption of vessels, quay cranes (QCs), yard cranes (YCs), reefers, and automated guided vehicles (AGVs) on the demand side. On the supply side, the energy is purchased from the electricity grid. Various operational research problems are included to accurately describe the operations within the terminal. We consider different operations including ship scheduling at berths, QC assignment, AGV assignment, YC assignment, AGV charging, and reefer temperature control. Fig. 1 shows the energy and information flow between all the loads and the electricity grid. The information flows are controlled by the terminal operating system (TOS), while the electricity flows are coordinated by the energy management system (EMS). The terminal operating and energy management systems exchange information to match the operational and electrical requirements.

Five electric loads are considered in the problem, namely ships, QCs, YCs, AGVs and reefer containers in the yard. Ships consume energy through onshore power supply while berthed, with a constant consumption rate per hour. The energy consumption of the QCs and YCs depends on the handling rate (h_m) of each equipment m. The energy demand of AGVs materializes through the charging of the AGV batteries. All AGVs are modeled as one large battery that is depleted based on the handling rate of the AGVs.

The reefer containers consume the energy required for cooling. In the yard, all reefer containers are modeled as one large cold storage tank, with heat transfer to the ambient temperature. Container temperature is allowed to fluctuate between specific bounds. The number of reefers present in the yard is assumed to be constant.

In the model, N vessels arrive at the terminal over H hours. For every vessel, a start time S and a finish time F are decided, which results in the berthing duration. Each vessel has a specific container load of d that needs to be handled during berthing. As it is customary in berth assignment problems, a ship is allowed to berth if there is available space on the quay. Once berthed, a number of QCs, YCs and AGVs are assigned to the ship every hour to load and unload the containers. The handling rate p set is determined based on the minimum and maximum handling capacity of QCs, YCs and AGVs.

Demand response (DR) is defined as a tariff or program developed to motivate the change in energy consumption of end-users, in response to changes in the price of electricity over time, or to give incentive payments designed to induce lower electricity use at times of high market prices or when grid reliability jeopardized. The DR in the studied problem is classified as the economic-based DR, in which the system operator designs different tariff structures like real-time pricing (RTP), critical peak pricing (CPP), time-of-use (TOU), peak load pricing to motivate different types of users like residential, commercial, and industrial. The energy price is an important factor that influences how consumers allocate energy resources. Users can alter their energy consumption patterns as per the tariff structure and comfort requirements. The impact of different pricing schemes (no pricing, single pricing and real-time pricing) is investigated in the study (Palensky and Dietrich, 2011; Patnam and Pindoriya, 2021).

The problem contains sources of uncertainty, both in the supply and demand of electricity. The uncertainty in supply is presented by electricity prices, while the uncertainty in demand is presented by ship arrival times. Notably, the prices of electricity and the arrival times of ships are the most significant uncertainties when optimizing a container terminal's operations planning. The uncertainty of the arrival times and electricity prices are considered to be independent of each other.

We formulate the problem as a two-stage optimization problem with uncertainties taken into account. The first stage decisions are taken one day ahead of when the operations are performed. A baseline schedule is created where the expected start time S_i^{da} for every vessel and the expected energy consumption P_t^{da} for every hour are decided upon in the first stage. The decisions in the second stage are made in real time just before performing the operations. The baseline decision made in the first stage can be changed by deciding upon berthing start time in scenario w ($S_{i,w}$) and power used in scenario w ($P_{t,w}$). The second stage objective is based on the expected value of all the different realizations. Different weights π_ξ are assigned to every realization based on the likelihood of occurrence.

A time step of one hour is considered in this model. Electricity prices from the market one day ahead of the actual operations are obtained every hour. Additionally, the energy demand of different loads is averaged over an hour assuming a constant consumption within one hour. For every hour, the amount of energy consumed is equal to the amount of energy supplied by the grid.

The real-time pricing model is present today (in e.g., Germany, or the Netherlands) under the name of dynamic pricing. If an energy customer opts for a dynamic pricing (what we call real-pricing in our paper) they will be exposed to the hourly wholesale market price. In this case, the customer is exposed to the fluctuations of the electricity price at the national level and will be required to remunerate their consumed energy under such fluctuating price. In contrast, what we call single-pricing scheme is a fixed-price contract for a certain duration of time. When the customer chooses a fixed-price contract they have a guaranteed price for every unit of energy they consume.

To explore the impact of DR, we compare the ship berthing schedule, energy consumption patterns and other related variables under the real-time pricing (time-variant pricing during the planning horizon) scheme with those under no-pricing and single-pricing schemes. No pricing scheme excludes cost-related factors when modeling, and the single-pricing scheme applies a single energy price for the entire day. The no pricing and single pricing schemes therefore do not include uncertain considerations. On the contrary, the real-time pricing scheme employs different energy prices for each time unit (usually hour) and considers uncertainty presented by energy prices in various scenarios.

The objective is to minimize the ship's lateness costs and energy-related costs. Deviations from the baseline schedule are minimized by considering rescheduling costs and power imbalance costs.

4. Mathematical model

4.1. Assumptions

The following assumptions are made in this problem:

(1) Ships only use constant onshore power when they are berthed.
(2) The berthing location of a ship does not influence energy consumption.
(3) The hoisting and lowering operations of QCs consume the same amount of energy for each container, which is the same case for YCs.
(4) The energy consumption of QCs, YCs and AGVs only depends on the handling rate.
(5) The number of reefers in the yard is constant throughout the day.
(6) The reefer cooling requirements are the same for every reefer container.
(7) All the reefer containers in the storage yard can be modeled as a large reefer container.
(8) The reefer energy consumption is based on the constant ambient temperature per time period.
(9) The AGV fleet can be modeled with one large battery.
(10) The energy consumption of the container terminal does not influence the electricity price.

4.2. Model formulation

In this section, a mixed-integer linear programming model is formulated for the problem described above. Tables 3, 4 and 5 present an overview of all sets, parameters and decision variables used in the model.

The objective function consists of scheduling and energy-related costs. The first two components of the objective function in Eq. (2) minimize the cost of lateness for all ships ($\sum_{i\in V} c_i^{late} L_{i,w}$) and the cost associated with deviations from the baseline schedule ($\sum_{i\in V} c^{resch} c_i^{late}$ $(S_{i,w}^{late} + S_{i,w}^{early})$). The subsequent two elements aim to minimize the cost connected to energy purchase on the day-ahead market ($\sum_{t\in T} c_{t,w}^{da} P_t^{da}$) and the cost associated with power imbalances in both shortage and surplus ($\sum_{t\in T} c_{t,w}^{da}(c^{shor} P_{t,w}^{shor} - c^{sur} P_{t,w}^{sur})$). These costs are calculated for each scenario and the weighted average of all scenarios is minimized.

$$\min_{V,T} \sum_{w\in S} \pi_w \left(\sum_{i\in V} c_i^{late} L_{i,w} + \sum_{i\in V} c^{resch} c_i^{late} (S_{i,w}^{late} + S_{i,w}^{early}) + \sum_{t\in T} c_{t,w}^{da} P_t^{da} + \sum_{t\in T} c_{t,w}^{da} (c^{shor} P_{t,w}^{shor} - c^{sur} P_{t,w}^{sur}) \right) \tag{2}$$

The model is subject to the following set of constraints. Constraint (3) ensures the energy consumed by the ships, quay cranes (QCs), yard cranes (YCs), automated guided vehicle (AGV) charging, and reefer

Table 3
Sets.

Sets	Description
V	Set of vessels to be served, $i \in 1, 2, \ldots, N$, where N is the number of vessels to be served.
T	Set of time periods, $t \in 0, 1, \ldots, t^{max} - 1$, where t^{max} is the number of hours considered.
P_i	Set of possible handling rate pattern p that can be assigned to a ship $i \in V$.
M	Types of machinery present in the terminal, $m \in \{QC, YC, AGV\}$.
S	Set of scenarios, $w \in S$.

Table 4
Parameters.

Parameters	Description
k_m	The number of machinery $m \in M$ available.
h_m	Handling rate of machinery m in containers per hour.
d_i	The total demand of containers to be handled (loaded + unloaded) for ship $i \in V$.
$u_{p,m}$	The number of machinery of type m used in handling rate pattern p.
l_i^{ship}	The quay length that ship i takes up.
l^{total}	The total length of the quay.
eat_i	Expected arrival time of vessel $i \in V$.
eft_i	Expected berthing finishing time of vessel $i \in V$.
$a_{i,w}$	Actual arrival time of vessel $i \in V$ in scenario $w \in S$.
e^{ship}	Energy consumption of a ship for onshore power for one hour.
$e_m^{machinery}$	Energy consumption of machinery m for operating for one hour.
e^{charge}	Energy consumed by one charger when charging an AGV every time unit.
$e^{charge,max}$	Maximum energy consumed by all chargers when charging AGVs every time unit.
b^{min}	Minimum battery level allowed for an AGV.
b^{max}	Maximum battery level allowed for an AGV.
η^{charge}	Charging efficiency.
$e^{reefer,max}$	Maximum energy consumption of all reefer connections every time unit.
tc^{min}	Minimum temperature allowed for reefer containers.
tc^{max}	Maximum temperature allowed for reefer containers.
η^{reefer}	Cooling efficiency.
ta_t	Ambient temperature at time period t.
m	Mass of the reefer.
cp	Specific heat capacity of a reefer.
u	Heat transfer coefficient of a reefer.
a	Area of the reefer.
$c_{t,w}^{da}$	Hourly electricity price at time period t in scenario w.
c_i^{late}	Penalty cost of exceeding the expected finishing time (EFT) for vessel $i \in V$ for one hour.
c_i^{resch}	Cost of changing the initial schedule by one hour, a coefficient multiplying c_i^{late}.
c^{sur}	Cost of having a surplus of energy, a coefficient multiplying $c_{t,w}^{da}$.
c^{shor}	Cost of having a shortage of energy, a coefficient multiplying $c_{t,w}^{da}$.
M	A large positive number.
π_w	Probability of scenario w's realization.

Table 5
Decision variables.

Decision variables	Description
$S_i^{da} \in \mathbb{Z}^+$	Scheduled berthing start time of vessel $i \in V$ in the baseline plan.
$S_{i,w} \in \mathbb{Z}^+$	Berthing start time of vessel $i \in V$ in scenario $w \in S$.
$S_{i,w}^{early} \in \mathbb{Z}^+$	Time the vessel $i \in V$ arrives ahead of schedule in scenario $w \in S$.
$S_{i,w}^{late} \in \mathbb{Z}^+$	Time the vessel $i \in V$ arrives behind schedule in scenario $w \in S$.
$F_{i,w} \in \mathbb{Z}^+$	Berthing end time (time when handling ends) of vessel $i \in V$ in scenario $w \in S$.
$L_{i,w} \in \mathbb{Z}^+$	Lateness of operations for ship $i \in V$ in scenario $w \in S$.
$A_{i,t,w} \in \mathbb{B}$	1 if vessel $i \in V$ is assigned at to a berth in time period t in scenario $w \in S$, 0 otherwise.
$H_{i,p,t,w} \in \mathbb{B}$	1 if pattern p of quay cranes, yard cranes and AGVs is assigned to serve vessel $i \in V$ at time period t in scenario $w \in S$, 0 otherwise.
$B_{t,w} \in \mathbb{R}^+$	Battery level at time period t in scenario $w \in S$.
$TC_{t,w} \in \mathbb{R}$	Reefer temperature at time period t in scenario $w \in S$.
$E_{t,w}^{charge} \in \mathbb{R}^+$	Energy consumed to charge AGVs at time period t in scenario $w \in S$.
$E_{t,w}^{reefer} \in \mathbb{R}$	Energy consumed to cool the reefers at time period t in scenario $w \in S$.
$P_{t,w} \in \mathbb{R}^+$	Power used from the utility grid at time period t in scenario $w \in S$.
$P_t^{da} \in \mathbb{R}^+$	Power purchased at the day-ahead market for time period t in the baseline plan.
$P_{t,w}^{sur} \in \mathbb{R}^+$	Power surplus at time period t in scenario $w \in S$.
$P_{t,w}^{shor} \in \mathbb{R}^+$	Power shortage at time period t in scenario $w \in S$.
$IM_{t,w}^{state} \in \mathbb{B}$	Imbalance state, 1 if there is a surplus and 0 if there is a deficit in scenario $w \in S$

cooling matches the power drawn from the grid.

$$\sum_{i\in V} e^{ship}\ A_{i,t,w} + \sum_{m\in M}\sum_{i\in V}\sum_{p\in P_i} u_{p,m}\ H_{i,p,t,w}\ e_m^{machinery} + E_{t,w}^{reefer} + E_{t,w}^{charge} = P_{t,w} \quad m = \{QC, YC\},\ \forall\ t\in T, \forall w\in S \tag{3}$$

Constraints (4)–(9) are associated with berth assignment of ships. Constraint (4) guarantees that the start time of vessel operation is either equal to or later than its expected arrival time. Constraint (5) defines the lateness time, which is the time a ship departs after the expected departure time. To ensure that the ships are berthed during every hour between the berthing start time and end time, Constraint (6), (7) and (8) are introduced. Constraint (9) prevents overcrowding of the berth by ensuring that the total length of all berthed vessels is shorter than the quay length.

$$S_{i,w} \geq a_{i,w} \qquad \forall i\in V, \forall w\in S \tag{4}$$

$$L_{i,w} \geq F_{i,w} - eft_i \qquad \forall i\in V, \forall w\in S \tag{5}$$

$$\sum_{t\in T} A_{i,t,w} = F_{i,w} - S_{i,w} \qquad \forall i\in V, \forall w\in S \tag{6}$$

$$(t+1)A_{i,t,w} \leq F_{i,w} \qquad \forall i\in V, t\in T, \forall w\in S \tag{7}$$

$$t\ A_{i,t,w} + t^{max}\ (1-A_{i,t,w}) \geq S_{i,w} \qquad \forall i\in V, t\in T, \forall w\in S \tag{8}$$

$$\sum_{i\in V} A_{i,t,w}\ l_i^{ship} \leq l^{total} \qquad \forall t\in T, \forall w\in S \tag{9}$$

Constraints (10)–(12) are related to the handling capacity assignment of cargo handling equipment. A handling rate is assigned to every ship for every hour it is berthed, which is accomplished by Constraint (10) and (11). Constraint (12) guarantees that the machinery capacity is not exceeded for QCs, YCs, and AGVs.

$$\sum_{p\in P_i} H_{i,p,t,w} = A_{i,t,w} \qquad \forall i\in V, t\in T, \forall w\in S \tag{10}$$

$$\sum_{t\in T}\sum_{p\in P_i} pH_{i,p,t,w} \geq d_i \qquad \forall i\in V, t\in T, \forall w\in S \tag{11}$$

$$\sum_{i\in V}\sum_{p\in P_i} u_{p,m}H_{i,p,t,w} \leq k_m \qquad \forall t\in T, m\in M, \forall w\in S \tag{12}$$

A day-ahead schedule is formulated for both the arrivals of the ships and power consumption. Constraint (13) states the difference between the actual start time in each scenario and the day-ahead scheduled start time is equivalent to the deviation of the start time. Similarly, Constraint (14) defines the energy consumption surplus and shortage. It is impossible to have a surplus and a deficit in energy consumption simultaneously. A binary variable $IM_{t,w}^{state}$ is used to keep track of whether there is a surplus or shortage, and Constraint (15) and (16) model this relationship.

$$S_{i,w}^{late} - S_{i,w}^{early} = S_{i,w} - S_i^{da} \qquad \forall i\in V, \forall w\in S \tag{13}$$

$$P_{t,w}^{shor} - P_{t,w}^{sur} = P_{t,w} - P_t^{da} \qquad \forall t\in T, \forall w\in S \tag{14}$$

$$P_{t,w}^{sur} \leq M \cdot IM_{t,w}^{state} \qquad \forall t\in T, \forall w\in S \tag{15}$$

$$P_{t,w}^{shor} \leq M \cdot (1 - IM_{t,w}^{state}) \qquad \forall t\in T, \forall w\in S \tag{16}$$

Constraints (17)–(19) concern the limits for energy used to charge AGVs and the AGV battery level. Constraints (17) and (18) describe that the total power used to charge the AGVs is constrained by the maximum energy limit and the number of AGVs available for charging. Constraint (19) ensures that the battery energy level always remains within the minimum and maximum allowed values.

$$E_{t,w}^{charge} \leq e^{charge,max} \qquad \forall t\in T, \forall w\in S \tag{17}$$

$$E_{t,w}^{charge} \leq (k_m - \sum_{i\in V}\sum_{p\in P_i} u_{p,m}\cdot H_{i,p,t,w})\cdot e^{charge} \quad m = \{AGV\},\ \forall t\in T,\ \forall w\in S \tag{18}$$

$$b^{min} \leq B_{t,w} \leq b^{max} \qquad \forall t\in T,\ \forall w\in S \tag{19}$$

Constraints (20)–(22) monitor the AGV battery level and guarantee the energy consumed equals the energy charged. Constraints (20) and (21) capture the principle that the state of battery charge fluctuates based on the amount of energy charged and discharged for time periods 1 to H and time period 0, respectively. We assume the initial battery level at the beginning is $(b^{min} + b^{max})/2$. Constraint (22) asserts that the amount of energy consumed equals the amount of energy charged.

$$B_{t,w} = B_{t-1,w} + \eta^{charge}\cdot E_{t,w}^{charge} - \sum_{i\in V}\sum_{p\in P_i} e_m^{machinery}\cdot u_{p,m}\cdot H_{i,p,t,w} \quad m = \{AGV\},\ \forall t\in T\setminus\{0\},\ \forall w\in S \tag{20}$$

$$B_{t,w} = (b^{min} + b^{max})/2 + \eta^{charge}\cdot E_{t,w}^{charge} - \sum_{i\in V}\sum_{p\in P_i} e_m^{machinery}\cdot u_{p,m}\cdot H_{i,p,t,w} \quad m = \{AGV\},\ t = \{0\},\ \forall w\in S \tag{21}$$

$$\sum_{t\in T}\eta^{charge}\cdot E_{t,w}^{charge} = \sum_{t\in T}\sum_{i\in V}\sum_{p\in P_i} e_m^{machinery}\cdot u_{p,m}\cdot H_{i,p,t,w} \quad m = \{AGV\},\ \forall w\in S \tag{22}$$

The following five constraints ensure the proper operation of the reefers. Constraint (23) indicates that the temperature of the reefers, represented by $TC_{t,w}$, should always be within the minimum and maximum temperature to ensure the good quality of the stored content. The energy consumed by the reefers at any time should not exceed the maximum rated power of all the reefer connections, as dictated by Constraint (24). The reefers lose heat to the environment through convection. This heat loss depends on the temperature difference between the container and the environment, both of which are assumed to be constant for every hour. Constraint (25) is the cooling balance constraint, which stipulates that the temperature change of the reefer container depends on the heat loss and the cooling energy supplied. Constraint (26) requires the same cooling balance for the initial time period. Constraint (27) is the reefer energy constraint, which ensures that the total energy lost through heat transfer equals the total energy consumed by cooling.

$$tc^{min} \leq TC_{t,w} \leq tc^{max} \qquad \forall t \in T, \forall w \in S \tag{23}$$

$$E^{reefer}_{t,w} \leq e^{reefer,max} \qquad \forall t \in T, \forall w \in S \tag{24}$$

$$m \cdot cp \cdot (TC_{t,w} - TC_{t-1,w}) = u \cdot a \cdot (ta_t - (tc^{min} + tc^{max})/2) - \eta^{reefer} \cdot E^{reefer}_{t,w} \qquad \forall t \in T \setminus \{0\}, \forall w \in S \tag{25}$$

$$m \cdot cp \cdot (TC_{t,w} - (tc^{min} + tc^{max})/2) = u \cdot a \cdot (ta_t - (tc^{min} + tc^{max})/2) - \eta^{reefer} \cdot E^{reefer}_{t,w} \qquad t = \{0\}, \forall w \in S \tag{26}$$

$$\sum_{t \in T} u \cdot a \cdot (ta_t - (tc^{min} + tc^{max})/2) = \sum_{t \in T} \eta^{reefer} \cdot E^{reefer}_{t,w} \qquad \forall w \in S \tag{27}$$

These constraints manage the energy consumption of ships, QCs, YCs, AGVs and reefer containers while adhering to the constraints based on the operations planning. We also add the domains of all variables in Table 5.

5. Solution procedure

This section explains the algorithmic procedure to obtain the solutions. First, the stochastic decomposition method, progressive hedging, is introduced. Then, we explain how the scenarios are obtained.

5.1. Stochastic decomposition with progressive hedging

Optimization problems under uncertainty are notoriously complex to solve, both in theory and practice. A practical method to tackle these problems involves the use of decomposition strategies in stochastic programming models. This process breaks down the overarching issue into manageable sub-problems, simplifying the overall optimization process and reducing computational complexity.

To handle this complexity efficiently, we implement a progressive hedging (PH) algorithm based on the original PH algorithm introduced by Rockafellar and Wets (1991). The algorithmic steps are shown presented in pseudo-code in Algorithm 1. The PH algorithm is based on the split-variable formulation of Formulation (1), which can be compactly written as Formulation (28).

$$\min \quad f^F(\boldsymbol{x}_\xi) + \mathbb{E}_P[q(\boldsymbol{y}_\xi, \xi)] \tag{28a}$$

$$\text{s.t.} \quad \boldsymbol{A}\boldsymbol{x}_\xi = \boldsymbol{b}, \quad \forall \xi \in \Xi \tag{28b}$$

$$\boldsymbol{T}_\xi \boldsymbol{x}_\xi + \boldsymbol{W}_\xi \boldsymbol{y}_\xi = \boldsymbol{h}_\xi, \quad \forall \xi \in \Xi \tag{28c}$$

$$\boldsymbol{x}_\xi - \bar{\boldsymbol{x}} = 0, \quad \forall \xi \in \Xi \tag{28d}$$

The PH algorithm is a practical way for splitting a large problem into smaller sub problems and solving them iteratively, thus possibly reducing the solving time considerably. The idea of the PH algorithm is to aggregate the solutions of subproblems, where artificial costs have been added. These added costs enforce that the aggregated solutions become non-anticipative and are updated in every iteration of the algorithm. The non-anticipativity constraint (28d) enforces that all the decisions taken in the first stage must be the same under all scenarios. The PH algorithm is based on the idea of relaxing the non-anticipativity constraint, solving all scenario subproblems separately and then iteratively achieving consensus on the non-anticipative first-stage solution. The mathematical model presented in Formulation (1) is decomposed into several independent optimizations for every scenario, with $\boldsymbol{x}^{v}_{\xi}, \boldsymbol{y}^{v}_{\xi}$ representing the decision variable of the first and second stage, respectively. $\boldsymbol{x}^{v}_{\xi}$ includes S^{da}_{i} and P^{da}_{t} in this model, and $\boldsymbol{y}^{v}_{\xi}$ represents all the other decision variables.

Algorithm 1 first sets the initial value for iteration counter v and penalty parameter $\rho > 0$, and then solves the model for the first time. The initial mean value of $\boldsymbol{x}_\xi$ and the initial dual prices are calculated. In the following steps, the mathematical model of this problem is iteratively solved, with the mean value of $\boldsymbol{x}_\xi$ and dual prices λ_ξ (also called Lagrange multipliers) updated in every interaction. The model is solved in parallel for each scenario. The dual price is represented by λ^{v}_{ξ} and the likelihood of occurrence of every scenario is represented by π_ξ. ρ is the penalty experienced for deviations of the first-stage decision variable from the mean. The core idea of progressive hedging can be motivated via the augmented Lagrangian method, which combines classical Lagrangian methods and the penalty function. The problem is solved iteratively for v times until sufficient convergence of $\sum_{\xi \in \Xi} \pi_\xi \|\boldsymbol{x}^{(v+1)}_{\xi} - \bar{\boldsymbol{x}}^{(v+1)}\|_2 < \delta_0$ is met or the maximum number of iterations reaches.

5.2. Scenario generation

Generating and reducing scenarios accurately is crucial in stochastic programming. For efficiency and accuracy, a balance between sample size and complexity is sought, with a preference for the least number of samples (Roald et al., 2023).

For ship arrival times, we observed historical data and found that the estimated arrival time generally follows a uniform distribution. A quasi-random sampling technique, specifically Halton sampling, was utilized to get distinct scenarios. The arrival distribution was obtained from Kolley et al. (2023). The actual arrival time is generated by adding uniformly distributed estimated arrival time plus the deviation time obtained from quasi-random sampling that conforms to a normal distribution. This method promotes a uniform distribution and distinct scenarios, leading to more accurate optimization results. The arrival times were rounded to the nearest hour, with corresponding probabilities for each hour.

In terms of electricity price scenarios, an approach based on the clustering method in Crespo-Vazquez et al. (2018) was used. Using historical data from the German day-ahead market, a K-means clustering algorithm was implemented to group days with similar prices. We use the day with the median value in each cluster to represent each cluster, with cluster weights derived from normalizing the number of days in each cluster.

Upon obtaining the individual scenarios for both the arrival times and electricity prices, the total set of scenarios was generated using the Cartesian product of the two sets. The associated probability for each scenario was obtained as the product of the probabilities of arrival time and electricity prices. This method led to a near-actual representation of uncertainty and less computational time for the optimization model.

We conduct computational experiments in the next section. We use the data collected from the open platform or website of HHLA Container Terminal Altenwerder (CTA) in Port of Hamburg to run various experiments and analyze the results. Details are further explained in the next section.

6. Computational experiments and results

This section conducts computational experiments and presents the results obtained. To find the potential for demand response, we present a case study of the HHLA Container Terminal Altenwerder (CTA) in Hamburg. Altenwerder is a state-of-the-art container terminal with a high degree of automation and has a lot of electrified equipment. Additionally, CTA has much data publicly available.

Algorithm 1: Progressive hedging for a two-stage stochastic optimization

Initialization: Let the iteration counter $\nu = 0$, the penalty parameter ρ;
Solve the scenario subproblems for each $\xi \in \Xi$:

$$\boldsymbol{x}_\xi^{(0)}, \boldsymbol{y}_\xi^{(0)} = \underset{\boldsymbol{x}_\xi, \boldsymbol{y}_\xi \in \boldsymbol{X}(\xi)}{\arg\min} \quad f^F(\boldsymbol{x}_\xi) + f^S(\boldsymbol{x}_\xi, \boldsymbol{y}_\xi, \xi)$$

Compute the initial solution $\bar{\boldsymbol{x}}^{(0)} = \sum_{\xi \in \Xi} \pi_\xi \boldsymbol{x}_\xi^{(0)}$ and the initial duals:

$$\lambda_\xi^{(0)} = \rho(\boldsymbol{x}_\xi^{(0)} - \bar{\boldsymbol{x}}^{(0)}), \quad \forall \xi \in \Xi$$

while $\sum_{\xi \in \Xi} \pi_\xi \|\boldsymbol{x}_\xi^{(\nu+1)} - \bar{\boldsymbol{x}}^{(\nu+1)}\|_2 \geq \delta_0$ *or* $\nu \leq \nu_{max}$ **do**

Solve the augmented scenario subproblems for all $\xi \in \Xi$:

$$\boldsymbol{x}_\xi^{(\nu+1)}, \boldsymbol{y}_\xi^{(\nu+1)} = \underset{\boldsymbol{x}_\xi, \boldsymbol{y}_\xi \in \boldsymbol{X}(\xi)}{\arg\min} \quad f^F(\boldsymbol{x}_\xi) + f^S(\boldsymbol{x}_\xi, \boldsymbol{y}_\xi, \xi) + \lambda_\xi^{(\nu)} \boldsymbol{x}_\xi + \frac{\rho}{2} \|\boldsymbol{x}_\xi - \bar{\boldsymbol{x}}^{(\nu)}\|_2^2$$

Solution update:

$$\bar{\boldsymbol{x}}^{(\nu+1)} = \sum_{\xi \in \Xi} \pi_\xi \boldsymbol{x}_\xi^{(\nu+1)}$$

Duals update:

$$\lambda_\xi^{(\nu+1)} = \lambda_\xi^{(\nu)} + \rho(\boldsymbol{x}_\xi^{(\nu+1)} - \bar{\boldsymbol{x}}^{(\nu+1)}), \quad \forall \xi \in \Xi$$

Iteration update: $\nu = \nu + 1$

end

The computations were all conducted using the commercial solver Gurobi v10.0.1, in combination with the Pyomo modeling language. For the stochastic decomposition, the mpi-sppy package was utilized (Knueven et al., 2020). The optimization model was run on an Intel i7-7700HQ processor with a 2.80 GHz clock speed and 8.00 GB of RAM.

All optimizations were solved using the progressive hedging algorithm. Ten iterations and a penalty parameter of 8000 were employed for each scenario's solution to converge. For all models, a mixed-integer programming optimality gap of 5% was used as a termination criterion. The solving time for each individual scenario was limited to 300 s. A convergence threshold of 0.01 was set. The convergence was lower than 0.01 for most of the experiments, though the threshold was not reached within 10 iterations in every experiment. The convergence metric was lower than 0.05 in all cases.

6.1. Model parameters

This section presents the parameters used in the study. We collected ship berthing record data from the open platform HHLA COAST. The sailing list from the CTA revealed that between April 10, 2023 and May 7, 2023, 190 ships arrived at the CTA terminal, averaging 7 ships per day (HHLA, 2025b). The terminal equipment configuration data was collected on the CTA website. The terminal utilizes 14 quay cranes (QCs), 74 battery electric automated guided vehicles (AGVs), and 52 yard cranes (YCs) for container handling (HHLA, 2025a). Containers are delivered and dispatched via ship, truck, or train. No onshore power facilities are currently applied at the CTA terminal. The length of the quay at CTA is found to be 1400 m (HHLA, 2025a). Based on the container layout, it is estimated that the AGVs travel an average distance of 947 m in 237 s to move a container (Zhang et al., 2023). Currently, there are 18 charging stations with a combined capacity of 4 MW for these AGVs (HHLA, 2025c).

The energy consumption for QCs and YCs to move one container is estimated to be 8 kWh and 2 kWh, respectively (He, 2016; He et al., 2015a; Iris and Lam, 2021). Additionally, the handling speed of both QCs and YCs is set to 30 containers per hour (He, 2016; He et al., 2015a). The average energy consumption of AGVs per meter is 0.00935 kWh (He et al., 2015b). By multiplying the energy consumption per meter with the average travel distance, the energy consumption for AGVs is estimated to be 9 kW per container move. Furthermore, based on the travel time, the handling rate for the AGVs is calculated to be 15 containers per hour.

Three types of ships are assumed to arrive at the container terminal: feeder, short-sea, and deep-sea vessels. Following the work of Iris and Lam, it is assumed that 40% of ships are feeders, 40% are short-sea vessels, and 20% are deep-sea vessels (Iris and Lam, 2021). The ship lengths are uniformly distributed in the ranges [70, 200] for feeders, [210, 300] for short-sea vessels, and [300, 400] for deep-sea vessels (Iris and Lam, 2019a). The container demand is also assumed to be uniformly distributed in the ranges [200, 600] for feeders, [600, 1600] for short-sea vessels, and [1600, 4500] for deep-sea vessels (Iris and Lam, 2021). Based on the number of QCs, YCs, and AGVs assigned to fulfill the demand, the ship unloading rate varies. The handling rate is defined as the handling speed multiplied by the number of QCs, YCs, and AGVs assigned. For feeders, the handling rate can be one of 30, 45, 60, for short-sea vessels 60, 75, 90, 105, 120, and for deep-sea vessels 120, 135, 150, 165, 180.

The estimated time of arrival for each ship is distributed uniformly in the range [0, 24]. The actual arrival time $a_{t,\omega}$ is the estimated arrival time plus a deviation, which is different for every scenario. The arrival time deviations are normally distributed with a mean of 0 and a standard deviation of 3 h, similar to Kolley et al. (2023). The estimated time of finishing is calculated by dividing the container demand by the minimum handling rate and adding the estimated time of arrival. If a ship departs later than the estimated finishing time, a penalty is applied. This penalty is obtained by converting the penalty stated by Iris and Lam (2021) to euros, assuming an exchange rate of 0.63 euro/SDG, resulting in penalties of 630 euros, 1260 euros, and 1890 euros for feeder, short-sea, and deep-sea vessels, respectively. Additionally, a penalty of 20% of the late penalty is assumed with regards to changing the berthing schedule created on the previous day, similar to the approach used by Liu et al. (2020).

For the energy consumption of reefer containers, it is assumed that all reefers are of the same type. According to a breakdown by van Duin et al. (2018), frozen product-based reefer containers are the most common type. The temperature range allowed for frozen products like meat and fish is between −20 and −16 °C (van Duin et al., 2018). Based on the average values for a 40 ft container, the mass, specific heat, heat transfer coefficient, and area of a reefer container are 24 500 kg, 2.76 $\text{kJ/kg} \cdot \text{K}$, 0.4 $\text{W/m}^2 \cdot \text{K}$, and 135.26 m^2, respectively (Kanellos, 2017). A cooling efficiency of 0.95 and the maximum cooling power are obtained from Kanellos (2017). At the CTA terminal, there are 2200 reefer connections, of which it is assumed that an average of 1500 are used simultaneously (HHLA, 2025a).

According to the HHLA website, it takes 1.5 h to charge one AGV (HHLA, 2022). Based on the charging rate and the number of AGVs, it can be calculated that all AGVs together can store 24.7 MWh of electricity. A charging efficiency of 90% is assumed, similar to Kanellos (2017).

Historical electricity prices from the day-ahead market in Germany were obtained from the ENTSO-E (2025) website. A penalty of 20% of the day-ahead price was assumed for having an energy surplus or shortage, following the approach of Crespo-Vazquez et al. (2018). The maximum allowed imbalance was set to 10 MW.

While the current experiments focus on a single-terminal system, we note that the model has been successfully executed for instances involving up to 40 vessels within a 48-h horizon, well above the typical daily number of ships for this container terminal. This suggests that the current model is, to some extent, suitable for larger terminal systems.

In the case of multi-terminal port systems, however, additional model adjustments would be necessary to reflect the structural and operational relationships between terminals, such as whether their energy systems are jointly managed or independently operated. These extensions would primarily affect the constraints and can be integrated into the existing framework.

6.2. The impact of stochastic modeling

The mathematical formulation of the stochastic problem (SP) is given by Formulation (1). We consider the uncertainty in the arrival times of ships and electricity prices. To find the impact that stochastic modeling has on the results, a comparison is made between the stochastic problem (SP) and several reactive approaches. For reactive approaches, the first-stage variables of the stochastic problem are fixed at some specific values. The mathematical formulation of the reactive approach is given in Eq. (29). In the problem described in Section 3, the first-stage variables are the start time of operations, S_i^{da}, and the energy purchased on the day-ahead market, P_t^{da}. Three reactive approaches are formulated, RE(reactive problem), RE+ and EEV(expectation of the expected value problem). For the RE and RE+ approach, S_i^{da} is set to the estimated arrival time eat_i. P_t^{da} is set to 0 and the average daily consumption $\bar{P}^{da}$ for the RE and RE+ approach respectively. For the EEV, S_i^{da} and P_t^{da} are set to the solutions that can be obtained by solving the expected value problem. The mathematical formulation of the expected value problem is given by Eq. (30). The x obtained from this problem is then used as x_0 in Eq. (29).

$$\min_{\boldsymbol{x}_0, \boldsymbol{y}_\xi \in \boldsymbol{X}(\xi)} \quad f^F(\boldsymbol{x}_0) + \mathbb{E}_P[f^S(\boldsymbol{x}_0, \boldsymbol{y}_\xi, \xi)] \tag{29a}$$

$$\text{where} \quad \boldsymbol{x}_0 : \text{fixed} \tag{29b}$$

$$\min_{\boldsymbol{x}, \boldsymbol{y}_{\bar{\xi}} \in \boldsymbol{X}(\bar{\xi})} \quad f^F(\boldsymbol{x}) + f^S(\boldsymbol{x}, \boldsymbol{y}_{\bar{\xi}}, \bar{\xi}) \tag{30a}$$

$$\text{where} \quad \bar{\xi} = \mathbb{E}_P[\xi] \tag{30b}$$

For comparison, the results of the stochastic model can also be compared with the wait-and-see solution (WS). This solution gives a lower bound to the problem in case a perfect forecast of the first-stage decision variables is known. the wait-and-see solution is however not achievable in practice, since no perfect forecast exists. The mathematical formulation of WS is given by Eq. (31).

$$\min_{\boldsymbol{x}_\xi, \boldsymbol{y}_\xi \in \boldsymbol{X}(\xi)} \quad \mathbb{E}_P[f^F(\boldsymbol{x}_\xi) + f^S(\boldsymbol{x}_\xi, \boldsymbol{y}_\xi, \xi)] \tag{31}$$

Table 6
Result comparison among reactive approaches and stochastic problem

No.	RE Total cost [€]	RE+ Total cost [€]	EEV Total cost [€]	SP Total cost [€]
1	62 863.8	58 775.9	53 217.3	50 138.7
2	62 074.0	57 967.5	53 056.8	47 049.1
3	69 925.5	63 784.6	59 770.4	57 459.1
4	53 117.1	51 103.7	40 004.2	39 828.8
5	81 891.7	74 881.7	67 645.8	62 538.3
6	67 430.5	61 454.6	53 747.0	52 804.4
7	75 826.3	69 324.2	62 984.9	61 154.2
8	48 113.5	45 913.3	41 666.9	39 914.3
9	71 876.7	65 269.8	56 203.4	54 556.0
10	59 377.4	55 685.1	55 818.4	52 716.3
Avg	**65 249.7**	**60 416.1**	**54 411.5**	**51 815.9**
Cost savings (%)	**0.0**	**7.4**	**16.6**	**20.6**

Note: RE (Reactive problem), EEV (Expectation of the expected value problem), SP (Stochastic problem), Cost savings (%) = $(Avg_{RE} - x) * 100/Avg_{RE}$.

Table 6 gives the results of total costs for the RE, RE+, EEV and SP approaches. The optimization was done ten times for each approach, using different random seeds. For every approach, the cost reduction compared to the RE approach is calculated. The difference between the results from RE approach and results from other approaches (RE+, EEV, SP) is divided by the results from RE results to get the cost saving percentage. By employing the EEV strategy, a cost reduction of 16.6% can be achieved. The stochastic problem presented in this paper further increases the cost reduction to 20.6%. As for wait-and-see (WS) solution, the average cost for ten iterations is 44 096.5€. The hypothetical maximum reduction achievable through WS solution is 32.4%.

Based on the differences between the EEV and SP solutions, the value of the stochastic solution (VSS) is calculated using Eq. (32). Similarly, the expected value of perfect information (EVPI) is computed using Eq. (33), which represents the difference between the SP and WS solutions. As the equations below show, the stochastic approach we use is superior to the EEV, and there is also space for improving forecasting accuracy.

$$VSS = EEV - SP = 54411.5 – 51815.9 = 2595.6 \tag{32}$$

$$EVPI = SP - WS = 51815.9 – 44096.5 = 7719.4 \tag{33}$$

6.3. The positive impact of demand response

To assess the impact of demand response on the solution, we consider different electricity pricing schemes: no pricing (NP), single pricing (SP), and real-time pricing (RTP) cases.

In the NP case, all energy-related costs in the objective function are disregarded. The objective function is simplified by removing the energy cost terms, resulting in Eq. (34).

$$\min_{\mathbf{V},\mathbf{T}} \sum_{w \in \mathbf{S}} \pi_w \left(\sum_{i \in \mathbf{V}} c_i^{late} L_{i,w} + \sum_{i \in \mathbf{V}} c^{resch} c_i^{late} (S_{i,w}^{late} + S_{i,w}^{early}) \right) \tag{34}$$

In the SP case, the electricity price $c_{t,w}^{da}$ in the objective function is replaced with a single price $\bar{c}_w^{da}$ for each hour. The objective function is modified accordingly, resulting in Eq. (35). Therefore, there is no uncertainty in energy prices in this case.

$$\begin{aligned} \min_{\mathbf{V},\mathbf{T}} \sum_{w \in \mathbf{S}} \pi_w \Bigg(& \sum_{i \in \mathbf{V}} c_i^{late} L_{i,w} + \sum_{i \in \mathbf{V}} c^{resch} c_i^{late} (S_{i,w}^{late} + S_{i,w}^{early}) + \\ & \sum_{t \in \mathbf{T}} \bar{c}_w^{da} P_t^{da} + \sum_{t \in \mathbf{T}} \bar{c}_w^{da} (c^{shor} P_{t,w}^{shor} - c^{sur} P_{t,w}^{sur}) \Bigg) \end{aligned} \tag{35}$$

The mathematical formulation presented in Section 3 remains the same for the RTP case. However, for the SP and NP cases, minor adjustments are needed. Specifically, Constraint (22) and Constraint (27)

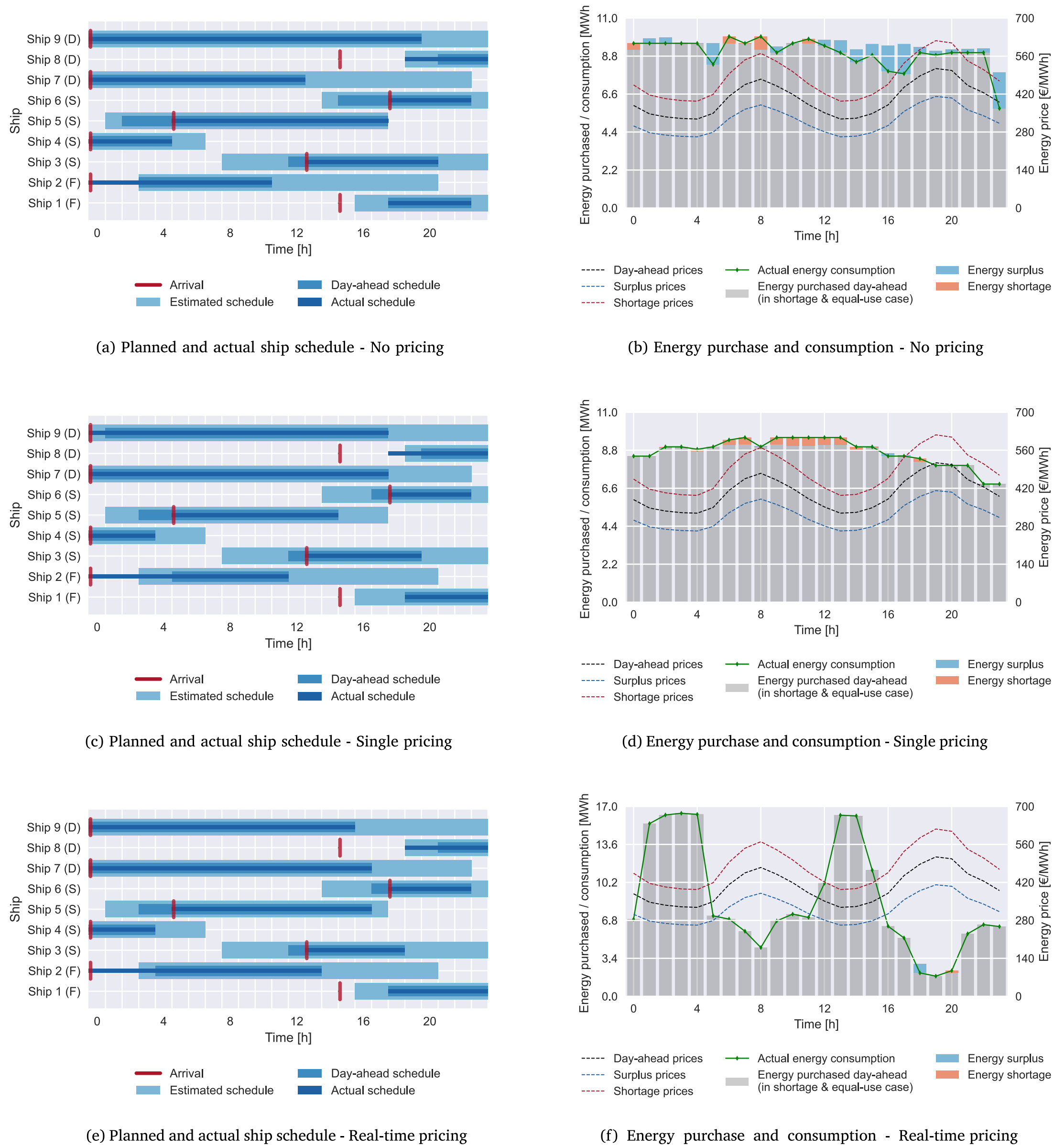

(a) Planned and actual ship schedule - No pricing

(b) Energy purchase and consumption - No pricing

(c) Planned and actual ship schedule - Single pricing

(d) Energy purchase and consumption - Single pricing

(e) Planned and actual ship schedule - Real-time pricing

(f) Energy purchase and consumption - Real-time pricing

Fig. 2. Ship schedule and hourly energy consumption of the second instance for different pricing strategies in the fourth scenario.

are replaced with Constraint (36) and Constraint (37), respectively. These changes ensure that the energy consumed by operations, such as charging and cooling, matches the energy demand for each time period without considering different prices. Constraint (36) and (37) prevent unnecessary rescheduling of charging and cooling times that would occur under the assumption of a single or no pricing scheme, as the timing of consumption becomes irrelevant in the SP and NP cases.

$$\eta^{charge} \cdot E^{charge}_{t,w} = \sum_{i\in V} \sum_{p\in P_i} e^{machinery}_{m} \cdot u_{p,m} \cdot H_{i,p,t,w} \quad (36)$$

$$m = AGV, \ \forall t \in T, \ \forall w \in S$$

$$u \cdot a \cdot (ta_t - (tc^{min} + tc^{max})/2) = \eta^{reefer} \cdot E^{reefer}_{t,w} \qquad \forall t \in T, \ \forall w \in S \quad (37)$$

Ten optimization experiments were performed for all three pricing schemes. Electricity prices of Germany in 2022 were used for the optimization.

Fig. 2 illustrates the planned and actual ship schedule and energy purchase and consumption for the second instance in the fourth scenario. By plotting the ship schedule and energy purchase and consumption, a visual comparison can be made between the different pricing strategies, including the decisions made in the first stage and how they changed in the second stage. In the subfigures for energy purchase and consumption, the grey bars represent the energy purchased one day ahead of the actual operations in the energy consumption shortage case (day-ahead energy purchase < energy consumption) or equal-use case (day-ahead energy purchase = energy consumption), while the stacked grey and blue bars represent day-ahead energy purchased in the energy consumption surplus case (day-ahead energy purchase > energy consumption).

For the NP alternative, power imbalances can be observed for most hours, resulting in higher energy costs. When the cost of electricity is taken into account in the SP alternative, these imbalances are significantly reduced, leading to lower energy costs. When the real-time pricing scheme (RTP scheme is implemented, imbalances occur much less frequently. Once real-time prices are considered in the optimization (RTP scenario), the energy consumption pattern also changes with the fluctuating prices. The energy consumption reduces during times of high prices, and the energy consumption increases during times of

Table 7
Result comparison of different pricing strategies.

No.	No pricing			Single pricing			Real-time pricing		
	EC [€]	SC [€]	TC [€]	EC [€]	SC [€]	TC [€]	EC [€]	SC [€]	TC [€]
1	44 628.1	13 482.0	58 110.1	43 325.8	13 692.0	57 017.8	38 798.7	11 340.0	50 138.7
2	49 746.6	6 804.0	56 550.6	47 013.8	6 602.4	53 616.2	42 317.8	4 731.2	47 049.1
3	53 979.6	11 390.4	65 370.0	50 921.5	10 735.2	61 656.7	47 429.5	10 029.6	57 459.1
4	45 266.7	3 931.2	49 197.9	39 856.1	4 989.6	44 845.7	35 544.8	4 284.0	39 828.8
5	57 095.3	11 793.6	68 888.9	55 677.2	11 844.0	67 521.2	52 357.5	10 180.8	62 538.3
6	55 265.5	3 376.8	58 642.3	52 559.4	4 737.6	57 297.0	48 559.9	4 244.5	52 804.4
7	55 561.2	10 533.6	66 094.8	52 899.1	9 626.4	62 525.5	48 999.4	12 154.8	61 154.2
8	46 231.0	4 284.0	50 515.0	40 303.2	3 780.0	44 083.2	35 991.5	3 922.8	39 914.3
9	54 584.0	8 618.4	63 202.4	51 742.4	6 442.8	58 185.2	47 626.0	6 930.0	54 556.0
10	50 439.0	9 651.6	60 090.6	45 624.5	8 794.8	54 419.3	41 401.5	11 314.8	52 716.3
Avg	**51 279.7**	**8 386.6**	**59 666.3**	**47 992.3**	**8 124.5**	**56 116.8**	**43 902.6**	**7 913.3**	**51 815.9**
Cost savings (%)	**0.0**	**0.0**	**0.0**	**6.4**	**3.1**	**5.9**	**14.4**	**5.6**	**13.2**

Note: EC (Energy-related cost), SC (Schedule-related cost), TC (Total cost), Cost savings (%) = $(Avg_{NP} - x) * 100/Avg_{NP}$.

low prices. We can find visible energy consumption peaks and troughs during planning horizon when applying real-time pricing scheme. Some differences in the berthing schedule can be observed between the different alternatives, although they are minor. Most of the differences are noticeable between the RTP scenario and the other two scenarios.

Table 7 presents the results of different pricing strategies, including NP, SP, and RTP. The costs are divided into energy-related costs and schedule-related costs. We assume that the percentage cost savings for different costs can be calculated directly using the costs obtained under different pricing methods. For example, the cost savings of energy-related costs can be directly calculated using the energy-related costs under different pricing schemes. The cost reduction compared to the results under no-pricing scheme is calculated. The difference between the results under the no-pricing scheme and results under other pricing schemes (single-pricing and real-time pricing) is divided by the results from no-pricing scheme to get the cost saving percentage. As the table shows, the real-time pricing strategy has a noticeable decrease in energy-related costs. By considering a single price or a real-time price of electricity, the energy-related costs decrease by 6.4% and 14.4%, respectively. It appears that scheduling costs also slightly decrease. However, the average absolute difference in scheduling costs between the no pricing and real-time pricing is small, at around 400 euros. It can be concluded that the real-time pricing scheme will have a relatively less significant impact on scheduling costs than it will have on energy-related costs, though no definitive conclusions can be drawn regarding the impact of energy-aware optimization on scheduling costs. By considering energy prices, the total operational cost of the terminal is reduced by 5.9% and 13.2% for the single and real-time pricing schemes, respectively, with energy-related costs accounting for the majority of the reduction. It shows that the real-time pricing scheme in a demand response mechanism performs well in the energy management system. This demonstrates that incorporating real-time pricing into terminal operations can yield substantial financial benefits. Moreover, the results highlight the importance of time-sensitive electricity pricing in improving cost-saving performance within demand response frameworks.

Fig. 3 displays the average energy consumption across all instances for the NP and RTP schemes. A negative correlation between energy consumption and electricity price is observed in the real-time pricing case. Compared to the steady consumption pattern during the planning horizon with the NP strategy, the average consumption increases at night and in the early afternoon when prices are lowest with the RTP scheme. This clear load-shifting behavior reflects how the model adapts energy usage in response to price signals, concentrating consumption in off-peak periods to reduce operational costs. The visual contrast between the two schemes illustrates the potential of real-time pricing scheme to reshape the temporal distribution of energy demand. To quantify this correlation, the Pearson correlation coefficient is calculated between energy consumption and electricity price. For the NP and SP schemes, a correlation of 0.09 and 0.03 is found, so almost no correlation exists between price and consumption. However, when RTP scheme is considered, the Pearson correlation coefficient becomes −0.85, indicating a strong negative correlation.

Furthermore, increased volatility in electricity consumption for RTP can be observed in Fig. 3. The peak-to-average ratio (PAR) is calculated for all different pricing schemes. The NP and SP schemes have PAR values of 1.17 and 1.19, respectively. In contrast, the RTP scheme exhibits a significantly higher PAR of 2.05. This means that the RTP strategy creates more volatile consumption with higher peaks. It is generally not desired since it causes more strain on the electricity grid.

Similarly to the energy demand, other decision variables can also be compared under different pricing schemes. Fig. 4 illustrates variations in the number of berthed ships, the handling rate of cargo handling equipment combination (QCs, YCs and AGVs), the power of AGV charging, and the power of reefer cooling. Each of these variables responds to price changes. A larger difference between NP and RTP indicates greater responsiveness of the variable to price changes. From Fig. 4, it can be visually observed that different variables change to a great extent when comparing the RTP and NP schemes. A metric called the flexibility coefficient (FC) is calculated to compare the sensitivity of each variable to price changes. The FC is defined as the standard deviation of the difference of variables between the NP and RTP schemes divided by the mean value of the variable under the NP scheme. The FC for each variable (X) can be calculated using Eq. (38). When comparing the FC for the variables above, we can discover that the cooling power is the most flexible, with a normalized standard deviation of 1.48. It implies that the rate at which reefers are cooled can be adjusted more readily in response to price changes. Following this, the AGV charging power also demonstrates notable flexibility. The handling rate and the number of ships berthed exhibit relatively lower levels of flexibility compared to other variables. These results suggest that energy-intensive and temporally shiftable components are more responsive to price signals. Understanding such flexibility can help operators identify the most effective levers for cost optimization under dynamic pricing schemes.

$$\mathrm{FC} = \frac{\sigma(X_{NP} - X_{RTP})}{\bar{X}_{NP}} \tag{38}$$

6.4. Price sensitivity

In light of the ongoing energy crisis in Europe, the electricity prices in 2022 were significantly higher compared to previous years. To assess the impact of demand response under different price scenarios, a sensitivity analysis is conducted.

To evaluate the influence of prices, the experiments described in Sections 6.2 and 6.3 were repeated using the price data from 2019. Since the energy prices were lower in 2019, the energy-related costs in 2022 exhibit a significant increase compared to the prices of 2019.

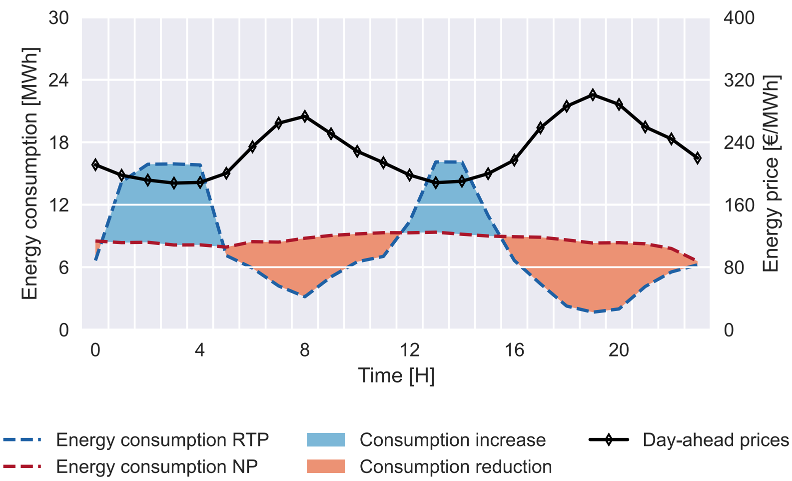

Fig. 3. Average energy consumption for No pricing and Real-time pricing schemes.

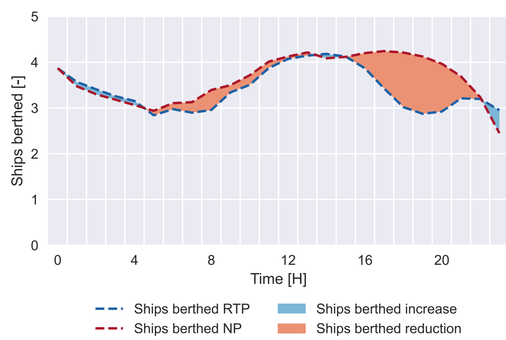

(a) Average number of ships berthed for NP and RTP schemes

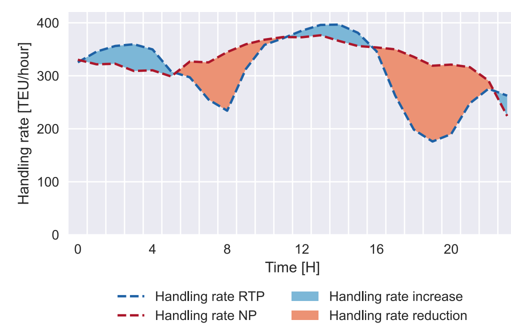

(b) Average handling rate of equipment combination for NP and RTP schemes

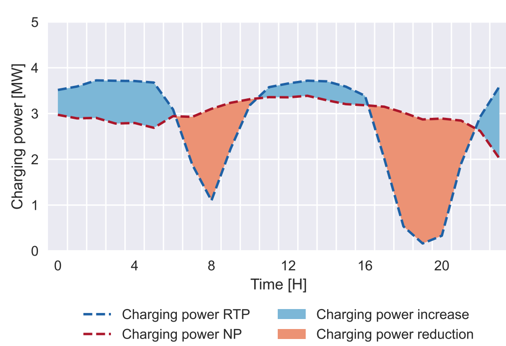

(c) Average AGV charging power for NP and RTP schemes

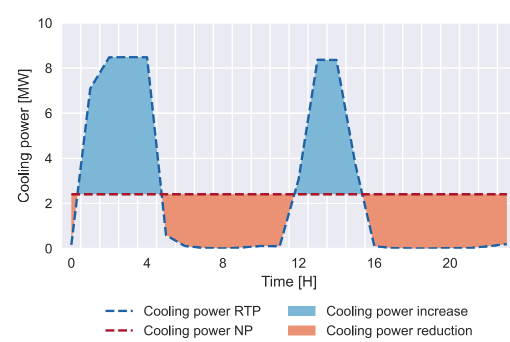

(d) Average cooling power for NP and RTP schemes

Fig. 4. Pattern comparison for different variables between No pricing and Real-time pricing schemes.

To further investigate the impact of rising electricity prices, the cost based on the real-time price scheme was calculated for each year from 2016 to 2022. For each year, ten instance experiments were conducted, and the average cost of all instances, as well as the cost increase compared to 2016, are shown in Table 8. It can be seen that due to the upward trend in electricity prices, the energy costs have increased by more than 800 percent since 2016. Consequently, the total costs have also risen significantly. Based on the computational experiments conducted in this study, no clear relationship can be observed between the scheduling costs and the rising electricity prices.

In summary, the sensitivity analysis highlights the considerable impact of electricity prices on the energy related costs and the overall cost of operations. The results underscore the importance of incorporating demand response strategies to mitigate the effects of fluctuating electricity prices and improve cost efficiency in port operations.

Table 8
Average cost comparison from 2016 to 2022.

Year	Average energy cost		Average schedule cost		Average total cost	
	€	%	€	%	€	%
2016	5124.8	100.0	7646.5	100.0	12 771.3	100.0
2017	6537.3	127.6	7208.2	94.3	13 745.6	107.6
2018	7604.0	148.4	7174.4	93.8	14 778.4	115.7
2019	5451.9	106.4	7252.5	94.8	12 704.4	99.5
2020	4418.7	86.2	7232.4	94.6	11 651.1	91.2
2021	29 074.0	567.3	7279.4	95.2	36 353.5	284.6
2022	43 902.6	856.7	7913.3	103.5	51 815.9	405.7

7. Managerial insights

The experimental results lead to several valuable managerial insights for the operations and management of container terminals. Focusing on the implications of energy-aware optimization on the operations, the following key insights emerge:

- The growing impact of uncertainty: Properly accounting for uncertainty in the demand and supply of energy is crucial when optimizing energy consumption and operations planning in container terminals. Failing to consider this uncertainty can result in up to 20% higher costs, on average, due to the need for subsequent operational plan changes.
- The economic opportunity of energy-aware planning: Implementing an energy-aware optimization approach based on hourly varying electricity prices can lead to significant cost reductions in container terminals, with potential savings of up to 13.2% of the operational costs. These cost savings can be achieved without requiring substantial investments in, for instance, energy storage or renewable energy infrastructure.
- The importance of real-time pricing: The real-time pricing scheme has a relatively more significant impact on energy-related costs than on scheduling costs. The inclusion of energy-related costs has a small impact on the scheduling costs. The decrease in energy-related costs accounts for the majority of the reduction in total costs.
- Container terminal (in this case, Alterwerder terminal) operators need to have more connection with grid operator/electricity power supplier to take care of the fluctuation of energy consumption, especially when consumption peaks and troughs happen.
- The role of peaks: The energy consumption peak period shifts with the implementation of the real-time pricing scheme. Energy consumption during peak periods is higher with real-time pricing than with the other pricing schemes. There is still space to explore the effect of real-time pricing on peak time-related electricity costs.
- The flexibility in energy consumption: To effectively manage the overall energy consumption of a container terminal, focusing on reefer container energy consumption holds the greatest potential with a flexibility coefficient of 1.48, followed by controlling the charging rate of AGVs, with a flexibility coefficient of 0.48. Furthermore, modifying the handling rate of ship (un)loading and adjusting ship arrival and departure times also have some potential to influence energy consumption throughout the day with a flexibility coefficient of 0.18 and 0.12, respectively.
- The model has the possibility to be extended to study the integration of renewable energy sources. The generation of renewable energy has a high degree of uncertainty, which can represent the uncertainty on the energy supply side. Different energy generation scenarios can be generated to be integrated into the stochastic programming model.

These insights highlight the potential for cost savings and operational improvements by considering electricity demand and implementing efficient control measures. By adopting these insights, container terminals can optimize their operations, reduce energy-related expenses, and get ready for the challenges of the transition to renewable energy sources.

8. Conclusions

8.1. Summary

Demand response (DR) is an effective measure to manage energy consumption and reduce energy-related costs in container terminals. It helps to adapt the power consumption of consumers in ports to better match the demand for power with the supply. Nonetheless, in academic literature, energy consumption management in ports has received limited attention, especially in the aspect of the uncertainty in energy demand and supply.

We present an integrated energy-aware optimization approach for the operations of a container terminal in this paper and build a stochastic programming model to formulate the operation and energy flow in container ports. The model considers vessels, quay cranes (QCs), yard cranes (YCs), reefers, and automated guided vehicles (AGVs) as multiple loads in the energy system. The uncertainty in demand is reflected in ship arrival times, and the uncertainty in supply is represented by electricity prices. We further develop a progressive hedging algorithm to efficiently solve the problem, and conduct computational experiments, based on data from Container Terminal Altenwerder (CTA) in the Port of Hamburg, to test the proposed model and explore its practical implications. The stochastic programming method proves to outperform reactive approaches consistently. We analyze different pricing strategies to assess the potential benefits of demand-responsive planning. Our results suggest the cost saving increases to 13.2% on average when applying real-time electricity prices, which is more than the cost saving achieved by the single pricing scheme. As for implications, our results show that considering uncertainty in the demand and supply of energy is crucial when optimizing energy consumption and operations planning in container terminals in an integrated way. Furthermore, we observe that implementing an energy-aware optimization approach based on hourly varying electricity prices can lead to significant cost reductions in container terminals, and including energy-related costs has minimal impact on the scheduling costs. Finally, the control of reefer energy consumption and adjusting the charging times of AGVs have the most potential to alter the overall energy consumption pattern.

8.2. Limitations and future research

The limitations of this study largely stem from the peaks and valleys of electricity consumption. The peaks may put pressure on the load of the grid, and the troughs may pose a challenge to the smooth operation of the grid. Considering the operational capacity of the grid linked to the port suggests a potential avenue for future research. In the future, researchers may explore peak and valley power for different loads and total energy requirements on grid capacity. Integrating the mechanism of the electricity grid into actual operational problems may lead to more realistic and instructive results. Extending the framework to include on-site renewable generation or energy storage systems offers a particularly promising avenue for future work, enabling joint optimization of stochastic generation, storage sizing and demand-response at the terminal scale. Moreover, incorporating carbon pricing or emissions-based penalties into the objective function — by linking energy consumption to time-varying emission intensities — could further enhance the environmental realism of the model and support carbon-aware operational planning.

CRediT authorship contribution statement

Jasper Stoter: Writing – original draft, Visualization, Validation, Software, Methodology, Investigation, Conceptualization. **Xinyu Tang:** Writing – review & editing, Supervision, Methodology. **Milos Cvetkovic:** Supervision, Conceptualization. **Peter Palensky:** Supervision. **Henk Polinder:** Supervision. **Çağatay Iris:** Writing – review & editing, Conceptualization. **Frederik Schulte:** Writing – review & editing, Supervision, Methodology, Conceptualization.

Declaration of Generative AI and AI-assisted technologies in the writing process

During the preparation of this work the author(s) used ChatGPT 4.0 in order to troubleshoot Python code and improve the text written for the paper. After using this tool/service, the author(s) reviewed and edited the content as needed and take(s) full responsibility for the content of the publication.

Declaration of competing interest

The authors declare that they have no known competing financial interests or personal relationships that could have appeared to influence the work reported in this paper.

Acknowledgment

This study was supported by the scholarship from China Scholarship Council (No. 202206230078).

Data availability

Data will be made available on request.

References

Bakar, N.N.A., Guerrero, J.M., Vasquez, J.C., Bazmohammadi, N., Yu, Y., Abusorrah, A., Al-Turki, Y.A., 2021. A review of the conceptualization and operational management of seaport microgrids on the shore and seaside. Energies 14 (23), 7941. http://dx.doi.org/10.3390/en14237941.

Crespo-Vazquez, J.L., Carrillo, C., Diaz-Dorado, E., Martinez-Lorenzo, J.A., Noor-E-Alam, M., 2018. A machine learning based stochastic optimization framework for a wind and storage power plant participating in energy pool market. Appl. Energy 232, 341–357. http://dx.doi.org/10.1016/j.apenergy.2018.09.195.

van Duin, J.H.R.R., Geerlings, H.H., Verbraeck, A.A., Nafde, T.T., 2018. Cooling down: A simulation approach to reduce energy peaks of reefers at terminals. J. Clean. Prod. 193, 72–86. http://dx.doi.org/10.1016/j.jclepro.2018.04.258.

ENTSO-E, 2025. ENTSO-E transparency platform. URL: https://transparency.entsoe.eu/.

Geerlings, H., Heij, R., van Duin, R., 2018. Opportunities for peak shaving the energy demand of ship-to-shore quay cranes at container terminals. J. Shipp. Trade 3 (1), 3. http://dx.doi.org/10.1186/s41072-018-0029-y.

Gennitsaris, S.G., Kanellos, F.D., 2019. Emission-aware and cost-effective distributed demand response system for extensively electrified large ports. IEEE Trans. Power Syst. 34 (6), 4341–4351. http://dx.doi.org/10.1109/TPWRS.2019.2919949, Conference Name: IEEE Transactions on Power Systems.

Grundmeier, N., Hahn, A., Ihle, N., Runge, S., Meyer-Barlag, C., 2014. A simulation based approach to forecast a demand load curve for a container terminal using battery powered vehicles. In: 2014 International Joint Conference on Neural Networks. IJCNN, (ISSN: 2161-4407) pp. 1711–1718. http://dx.doi.org/10.1109/IJCNN.2014.6889838.

Harnischmacher, C., Markefke, L., Brendel, A.B., Kolbe, L., 2023. Two-sided sustainability: Simulating battery degradation in vehicle to grid applications within autonomous electric port transportation. J. Clean. Prod. 384, 135598. http://dx.doi.org/10.1016/j.jclepro.2022.135598.

He, J., 2016. Berth allocation and quay crane assignment in a container terminal for the trade-off between time-saving and energy-saving. Adv. Eng. Informatics 30 (3), 390–405. http://dx.doi.org/10.1016/J.AEI.2016.04.006, Publisher: Elsevier Ltd.

He, J., Huang, Y., Yan, W., 2015a. Yard crane scheduling in a container terminal for the trade-off between efficiency and energy consumption. Adv. Eng. Informatics 29 (1), 59–75. http://dx.doi.org/10.1016/J.AEI.2014.09.003, Publisher: Elsevier Ltd.

He, J., Huang, Y., Yan, W., Wang, S., 2015b. Integrated internal truck, yard crane and quay crane scheduling in a container terminal considering energy consumption. Expert Syst. Appl. 42 (5), 2464–2487. http://dx.doi.org/10.1016/j.eswa.2014.11.016.

HHLA, 2022. Sustainability for container handling: AGV charging infrastructure completed. URL: https://hhla.de/en/media/news/detail-view/cta-agv-charging-infrastructure-completed.

HHLA, 2025a. Container Terminal Altenwerder (CTA). URL: https://hhla.de/en/company/subsidiaries/container-terminal-altenwerder-cta.

HHLA, 2025b. HHLA COAST report. URL: https://coast.hhla.de/report?id=Standard-Report-Segelliste.

HHLA, 2025c. Innovation: FRESH. URL: https://hhla.de/en/innovation/fresh.

Iris, Ç., Lam, J.S.L., 2019a. Recoverable robustness in weekly berth and quay crane planning. Transp. Res. Part B: Methodol. 122, 365–389. http://dx.doi.org/10.1016/j.trb.2019.02.013.

Iris, Ç., Lam, J.S.L., 2019b. A review of energy efficiency in ports: Operational strategies, technologies and energy management systems. Renew. Sustain. Energy Rev. 112, 170–182. http://dx.doi.org/10.1016/J.RSER.2019.04.069, Publisher: Pergamon.

Iris, Ç., Lam, J.S.L., 2021. Optimal energy management and operations planning in seaports with smart grid while harnessing renewable energy under uncertainty. Omega 103, 102445. http://dx.doi.org/10.1016/j.omega.2021.102445.

Kanellos, F.D., 2017. Real-time control based on multi-agent systems for the operation of large ports as prosumer microgrids. IEEE Access 5, 9439–9452. http://dx.doi.org/10.1109/ACCESS.2017.2706091.

Kanellos, F.D., 2019. Multiagent-system-based operation scheduling of large ports' power systems with emissions limitation. IEEE Syst. J. 13 (2), 1831–1840. http://dx.doi.org/10.1109/JSYST.2018.2850970.

Kanellos, F.D., Volanis, E.-S.M., Hatziargyriou, N.D., 2019. Power management method for large ports with multi-agent systems. IEEE Trans. Smart Grid 10 (2), 1259–1268. http://dx.doi.org/10.1109/TSG.2017.2762001.

Kermani, M., Parise, G., Martirano, L., Parise, L., Chavdarian, B., 2018. Optimization of peak load shaving in STS group cranes based on PSO algorithm. In: 2018 IEEE International Conference on Environment and Electrical Engineering and 2018 IEEE Industrial and Commercial Power Systems Europe (EEEIC / I&CPS Europe). pp. 1–5. http://dx.doi.org/10.1109/EEEIC.2018.8494467.

Knueven, B., Muir, C., Watson, J.-P., Mildebrath, D.T., Siirola, J.D., Woodruff, D.L., 2020. A parallel hub-and-spoke system for large-scale scenario-based optimization under uncertainty – optimization online. URL: https://optimization-online.org/2020/11/8088/.

Kolley, L., Rückert, N., Kastner, M., Jahn, C., Fischer, K., 2023. Robust berth scheduling using machine learning for vessel arrival time prediction. Flex. Serv. Manuf. J. 35 (1), 29–69. http://dx.doi.org/10.1007/s10696-022-09462-x.

Liu, C., Xiang, X., Zheng, L., 2020. A two-stage robust optimization approach for the berth allocation problem under uncertainty. Flex. Serv. Manuf. J. 32 (2), 425–452. http://dx.doi.org/10.1007/s10696-019-09343-w.

Mao, A., Yu, T., Ding, Z., Fang, S., Guo, J., Sheng, Q., 2022. Optimal scheduling for seaport integrated energy system considering flexible berth allocation. Appl. Energy 308, 118386. http://dx.doi.org/10.1016/j.apenergy.2021.118386.

Oyewola, O.M., Awonusi, A.A., Ismail, O.S., 2024. Performance optimization of step-like divergence plenum air-cooled li-ion battery thermal management system using variable-step-height configuration. Emerg. Sci. J. 8 (3), 795–814. http://dx.doi.org/10.28991/ESJ-2024-08-03-01.

Palensky, P., Dietrich, D., 2011. Demand side management: Demand response, intelligent energy systems, and smart loads. IEEE Trans. Ind. Informatics 7 (3), 381–388. http://dx.doi.org/10.1109/TII.2011.2158841.

Patnam, B.S.K., Pindoriya, N.M., 2021. Demand response in consumer-centric electricity market: Mathematical models and optimization problems. Electr. Power Syst. Res. 193, 106923. http://dx.doi.org/10.1016/j.epsr.2020.106923.

Pu, Y., Chen, W., Zhang, R., Liu, H., 2020. Optimal operation strategy of port integrated energy system considering demand response. In: 2020 IEEE 4th Conference on Energy Internet and Energy System Integration (EI2). pp. 518–523. http://dx.doi.org/10.1109/EI250167.2020.9346904.

Roald, L.A., Pozo, D., Papavasiliou, A., Molzahn, D.K., Kazempour, J., Conejo, A., 2023. Power systems optimization under uncertainty: A review of methods and applications. Electr. Power Syst. Res. 214, 108725. http://dx.doi.org/10.1016/j.epsr.2022.108725.

Rockafellar, R.T., Wets, R.J.-B., 1991. Scenarios and policy aggregation in optimization under uncertainty. Math. Oper. Res. 16 (1), 119–147.

Sarantakos, I., Nikkhah, S., Peker, M., Bowkett, A., Sayfutdinov, T., Alahyari, A., Patsios, C., Mangan, J., Allahham, A., Bougioukou, E., Murphy, A., Pazouki, K., 2024. A robust logistics-electric framework for optimal power management of electrified ports under uncertain vessel arrival time. Clean. Logist. Supply Chain 10, http://dx.doi.org/10.1016/j.clscn.2024.100144.

Schmidt, J., Lauven, L.-P., Ihle, N., Kolbe, L., 2015. Demand side integration for electric transport vehicles. Int. J. Energy Sect. Manag. 9 (4), 471–495. http://dx.doi.org/10.1108/IJESM-11-2014-0002.

Tang, G., Zhao, Z., Schulte, F., Iris, C., 2025. Smart charging with demand response and energy peak shaving for reefer containers with internet-of-things. Int. J. Prod. Res. 1–26. http://dx.doi.org/10.1080/00207543.2025.2499868.

Xiao, M., Zhou, Q., Zhang, Z., Yin, J., 2024. Real-time intrusion detection in power grids using deep learning: Ensuring DPU data security. HighTech Innov. J. 5 (3), 814–827. http://dx.doi.org/10.28991/HIJ-2024-05-03-018.

Xiong, C., Su, Y., Wang, H., Zhang, D., Xiong, B., 2024. Optimal distributed energy scheduling for port microgrid system considering the coupling of renewable energy and demand. Sustain. Energy, Grids Networks 39, http://dx.doi.org/10.1016/j.segan.2024.101506.

Yu, J., Voß, S., Song, X., 2022. Multi-objective optimization of daily use of shore side electricity integrated with quayside operation. J. Clean. Prod. 351, 131406. http://dx.doi.org/10.1016/j.jclepro.2022.131406.

Zhang, X., Gu, Y., Yang, Y., Liu, B., 2023. Comparing the efficiency of two types of yard layout in container terminals. Sustainability 15 (9), 7195. http://dx.doi.org/10.3390/su15097195.

Zhao, W., Ma, K., Yang, J., Guo, S., 2024. A risk-averse logistics-energy coordination optimization strategy for port energy system considering demand response program. Electr. Power Syst. Res. 231, http://dx.doi.org/10.1016/j.epsr.2024.110297.